whitesnake/sfpq Is Required for Cell Survival and Neuronal Development in the Zebrafish

Laura Anne Lowery, Jamie Rubin, and Hazel Sive*

Organogenesis involves both the development of specific cell types and their organization into a functional three-dimensional structure. We are using the zebrafish to assess the genetic basis for brain organogenesis. We show that the *whitesnake* mutant corresponds to the *sfpq* (splicing factor, proline/glutamine rich) gene, encoding the PSF protein (polypyrimidine tract-binding protein-associated splicing factor). In vitro studies have shown that PSF is important for RNA splicing and transcription and is a candidate brain-specific splicing factor, however, the in vivo function of this gene is unclear. *sfpq* is expressed throughout development and in the adult zebrafish, with strong expression in the developing brain, particularly in regions enriched for neuronal progenitors. In the *whitesnake* mutant, a brain phenotype is visible by 28 hr after fertilization, when it becomes apparent that the midbrain and hindbrain are abnormally shaped. Neural crest, heart, and muscle development or function is also abnormal. *sfpq* function appears to be required in two distinct phases during development. First, loss of *sfpq* gene function leads to increased cell death throughout the early embryo, suggesting that cell survival requires functional PSF protein. Second, *sfpq* function is required for differentiation, but not for determination, of specific classes of brain neurons. These data indicate that, in vertebrates, *sfpq* plays a key role in neuronal development and is essential for normal brain development. *Developmental Dynamics 236:1347–1357, 2007.* © 2007 Wiley-Liss, Inc.

Key words: *whitesnake*; *splicing factor proline glutamine rich*; PSF; zebrafish; brain development; neuronal determination; neuronal differentiation; cell death

Accepted 26 February 2007

INTRODUCTION

The development of organs is complex, involving both generation of appropriate cell types and tissues and organization of these in the correct three-dimensional structure. We have begun to examine brain organogenesis, using the zebrafish as a model and by studying mutants suggested to be defective in brain development (Jiang et al., 1996; Schier et al., 1996; Amsterdam et al., 2004).

The *whitesnake* (*wis*) mutant was isolated from a chemical mutagenesis screen, and shows a distinct brain phenotype (Jiang et al., 1996; Schier et al., 1996). Here, we show that the zebrafish *whitesnake* (*wis*) mutant corresponds to disruption of the *sfpq* gene. *sfpq* (*splicing factor*, *proline/glutamine rich*), which encodes the Polypyrimidine tract binding protein associated Splicing Factor (PSF), is enriched in differentiating neurons in the mouse brain and has been suggested to play a role in neural-specific splicing (Chanas-Sacre et al., 1999). PSF was first identified as an essential pre-mRNA splicing factor (Patton et al., 1993) and has since been shown to exhibit multiple functions in nucleic acid synthesis and processing in vitro and in tissue culture, including transcriptional corepression, DNA unwinding, and linking RNA transcripts with RNA polymerase II (Emili et al., 2002; Shav-Tal and Zipori, 2002). In addition, it has been suggested to play a role in tumorigenesis as well as apoptosis, as *sfpq* translocation occurs in papillary renal cell carcinoma (Clark et al., 1997), and nuclear relocaliza-

The Supplementary Material referred to in this article can be found at http://www.interscience.wiley.com/jpages/1058-8388/suppmat

Whitehead Institute for Biomedical Research, and Massachusetts Institute of Technology, Cambridge, Massachusetts

Grant sponsor: NIH; Grant Number: MH70926; Grant sponsor: NIH-NCRR; Grant number: RR12546; Grant sponsor: NIH NRSA.

***Correspondence to: Hazel Sive, Whitehead Institute for Biomedical Research, and Massachusetts Institute of Technology, Nine Cambridge Center, Cambridge, MA 02142. E-mail: sive@wi.mit.edu**

DOI 10.1002/dvdy.21132
Published online 28 March 2007 in Wiley InterScience (www.interscience.wiley.com).

tion and hyperphosphorylation of PSF occur during apoptosis (Shav-Tal et al., 2001).

In this report, we present the first whole animal study of *sfpq* loss of function. Our data suggest that *sfpq* function is required for cell survival and that it is also required for the differentiation, but not determination, of specific neuronal classes.

RESULTS AND DISCUSSION

The *whitesnake* Mutation Disrupts Normal Brain and Body Development

The *whitesnake* (*wis*) mutant was isolated from a chemical mutagenesis screen, and shows a distinct brain phenotype (Jiang et al., 1996; Schier et al., 1996). Phenotypic abnormalities are first visible during mid-somitogenesis. By 22 hr postfertilization (hpf), there is a subtle change in the curvature of the entire body, with the tail remaining more curved than wild-type siblings and the hindbrain more flat (not shown). In addition, *wis* mutants lack myotomal contractions, and the somites are abnormally organized (not shown). The *wis* phenotype is more pronounced by 24 hpf, with absence of eye pigmentation, and slightly reduced brain ventricle width (Fig. 1B,E). By 28 hpf, mutants show an absence or severe reduction in body pigmentation, flattening of the brain, a curved and thick yolk extension, reduced heartbeat, and a lack of touch response (Fig. 1H, and not shown). Injecting the brain cavity with a fluorescent dye (Lowery and Sive, 2005) highlights structural abnormalities by this stage—all the embryonic brain ventricles are reduced, with the midbrain ventricle most severely affected; however, there is variability in the extent of ventricle reduction (Fig. 1H and Supplementary Figure S1, which can be viewed at http://www.interscience.wiley.com/jpages/1058-8388/suppmat). At 2 days postfertilization (dpf), the *wis* brain is smaller than in wild-type siblings, and the size of all brain ventricle cavities are severely reduced, with the midbrain ventricle almost completely absent (Fig. 1J–Q). The tail does become straight, although all other 24 hours postfertilization (hpf) defects persist. *wis* mutant embryos die by 4 dpf, when cells appear to become necrotic and the embryo disintegrates. The two alleles analyzed, *tr241* and *m427*, have indistinguishable phenotypes.

These results show that loss of *wis* function leads to profound morphological defects affecting several organ systems, with specific defects in the brain. The brain morphology defect appears relatively late, after the initial shaping of the brain.

The *whitesnake* Mutant Corresponds to the *sfpq* Gene, Encoding the PSF Protein

We observed that the *wis* phenotype appears very similar to that of the *sfpq hi1779* retroviral insertion mutant (compare Fig. 1B and C, E and F, H and I), although only preliminary analysis of the *sfpq* phenotype has been reported (Amsterdam et al., 2004). The *sfpq* gene (Splicing Factor, Proline/glutamine (Q) rich) encodes the PSF (Polypyrimidine tract-binding protein-associated Splicing Factor) protein, a 619-amino-acid nuclear factor. In vitro assays using cell extracts indicate that PSF can participate in a variety of functions, including RNA splicing and transcriptional regulation (Patton et al., 1993; Shav-Tal and Zipori, 2002).

Crosses between the wis^{tr241} and *sfpq* mutants showed that they fail to complement, and are, therefore, likely to be different alleles of the same locus. In a cross of *wis* and *sfpq* heterozygotes, 144 (73%) showed a wild-type phenotype and 54 (27%) a mutant phenotype, as expected for noncomplementing loci (198 embryos total).

$sfpq^{hi1779}$ has a 6-kb retroviral insertion at base 553 in the coding sequence, which leads to a truncation of the protein at amino acid 197 (Fig. 1R). This truncation removes the RNA recognition motifs and the two nuclear localization sequences needed for protein function (Dye and Patton, 2001), suggesting that the *hi1779* PSF protein is not functional. We asked whether the *wis* phenotype is due to a mutation in the *sfpq* gene by comparing cDNA sequences from wild-type, wis^{tr241} and wis^{m427} mutants. The *tr241* allele of *wis* contains a C to T mutation at position 491 in the *sfpq* coding sequence, which results in a premature stop codon at amino acid position 167 (Fig. 1R) and severe truncation of the protein. The wis^{m427} allele has incorrect splicing of the last exon, which truncates the last 39 amino acids, removing the last nuclear localization sequence previously shown to be necessary for protein function (Dye and Patton, 2001). There are no obvious mutations in the wis^{m427} genomic DNA coding sequence that could account for the splicing error, and thus it is likely that the mutation exists elsewhere, perhaps in intronic sequence. We used reverse transcriptase-polymerase chain reaction (RT-PCR) to analyze *sfpq* RNA levels in wis^{m247} and did not see gross differences in levels between mutant and wild-type (data not shown).

We further confirmed gene assignment by rescuing the *wis* phenotype with *sfpq* mRNA. Injection of 100–200 pg of *sfpq* mRNA partially rescues the *wis* brain ventricle, yolk extension, pigment, and movement defects at 28 hpf (n = 17, 94% rescue, Fig. 2B,E, and Movie in Supplementary Materials). The incomplete rescue is likely to be due to degradation of the injected mRNA by later stages of development. Consistently, we were able to partially phenocopy the *wis* phenotype by injecting 8 ng of antisense morpholino oligonucleotides targeted to the *sfpq* start site (Fig. 2G–L). These morphant embryos showed the *wis* brain morphology defect, mild tail curvature, and reduced pigmentation in 100% of injected embryos (n = 89; Fig. 2H,K), although myotomal contractions and touch response were not eliminated, suggesting we were not able to completely deplete *sfpq* function with the morpholino.

sfpq Is Expressed Throughout the Embryo and Adult Zebrafish and Is Enriched in the Brain During Neuronal Development

PSF protein is localized to differentiating neurons in the embryonic mouse brain (Chanas-Sacre et al., 1999), but

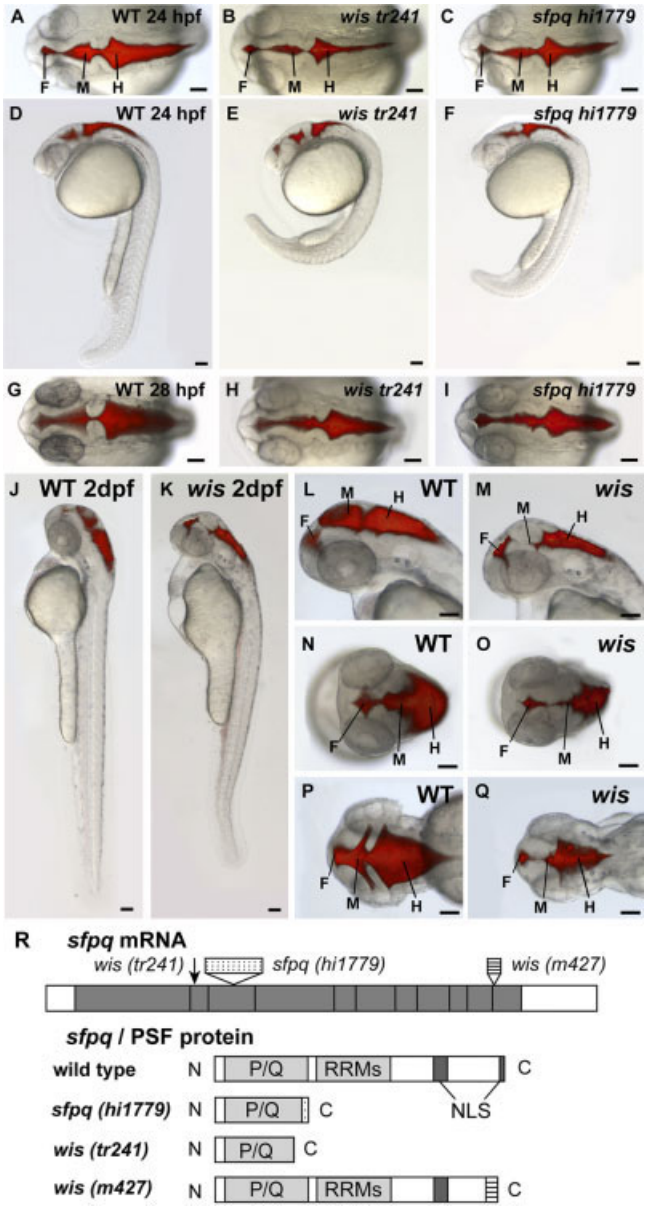

Fig. 1. Phenotype of *whitesnake/sfpq* mutants. **A–Q:** Brain ventricles were visualized by microinjecting a fluorescent dye, Rhodamine–dextran, into the hindbrain ventricle of living anesthetized embryos at 24 hours postfertilization (hpf, A–F), 28 hpf (G–I), and 2 dpf (J–Q). **A–F:** At 24 hpf, the *wis*^{tr241} mutant has reduced brain ventricles and abnormal curvature of the tail (B,E), as compared with wild-type (A,D), and the *sfpq*^{hi1779} mutant phenotype is similar (C,F). **G–I:** At 28 hpf, both *wis*^{tr241} and *sfpq*^{hi1779} show variable reduction in brain ventricle size and reduced pigmentation. **J–Q:** By 48 hpf, the *wis* brain ventricle reduction becomes more severe compared with wild-type, especially in the midbrain. A–C,G–I,N–Q: Dorsal views. D–F,J–M: Side views. F, forebrain; M, midbrain; H, hindbrain. Scale bar = 100 μm. **R:** *sfpq* gene/PSF protein and corresponding mutations. *wis*^{tr241} has a C to T mutation at position 491 of coding sequence, which results in an early stop codon at amino acid 167. *sfpq*^{hi1779} has a 6-kb retroviral insertion (which has a stop codon early in the insertion sequence). *wis*^{m427} mRNA has aberrant splicing resulting in 200 base pairs of intronic sequence inserted before the last exon. Both *sfpq*^{hi1779} and *wis*^{tr241} are truncated near the end of P/Q-rich region, and *wis*^{m427} lacks the last NLS. P/Q, proline/glutamine-rich region; RRMs, RNA recognition motifs; NLS, nuclear localization sequence.

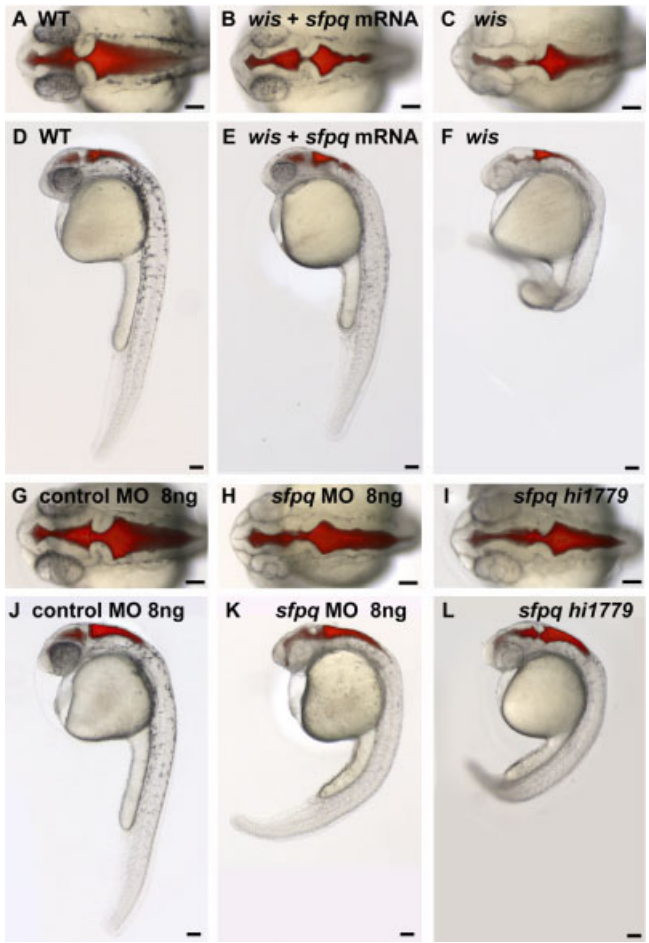

Fig. 2. *sfpq* mRNA partially rescues the *whitesnake* phenotype and *sfpq* morpholino phenocopies mutant phenotype at 28 hours postfertilization (hpf). **A–F:** Wild-type (WT) sibling of *wis*^{tr241} (A,D), *wis*^{tr241} mutant injected with ~100 pg *sfpq* mRNA (B,E), and *wis*^{tr241} mutant (C,F). **G–L:** WT injected with 8 ng of control morpholino (G,J), WT injected with 8ng *sfpq* morpholino (H,K), and *sfpq*^{hi1779} mutant (I,L). A–C,G–I: Dorsal views. D–F,J–L: Lateral views. Scale bar = 100 μm.

the expression pattern of this gene has not been thoroughly examined during development. We, therefore, examined the expression patterns and level of *sfpq* RNA during zebrafish development, using RT-PCR and whole mount in situ hybridization. RT-PCR shows that *sfpq* is expressed both maternally and zygotically, with maximal expression at 18 hpf and continuing through 3 dpf. Expression is also strong in the adult brain, but there are varying levels of weaker expression in the eyes, gut, heart, and body muscle (Fig. 3A). In situ hybridization demonstrates that *sfpq* expression is ubiquitous until mid-somitogenesis (Fig. 3B–G). By 18 hpf, *sfpq* expression is slightly stronger in presumptive rhombomere 4 (Fig. 3H, arrow) as

well as in the developing telencephalon (Fig. 3H, bracket). By 24 hpf, expression appears much stronger in the brain than in non-neural tissue (Fig. 3I), with strongest expression in the telencephalon, midbrain, hindbrain, and retina (Fig. 3J,K). At 2–3 dpf, *sfpq* expression is apparent only in distinct regions of the brain (Fig. 3L–Q). At 2 dpf, expression is strong in the ventral hindbrain and in dorsoventral stripes throughout the hindbrain (Fig. 3M,N). At 3 dpf, expression is strongly detected in a region ventral to the brain, but also faintly along many axon tracts (Fig. 3O–Q). By the more sensitive RT-PCR assay, *sfpq* is also expressed in the tail at 3 dpf (Fig. 3A, lane 9).

The strong expression of *sfpq* in distinct areas of the brain prompted us to ask whether this gene is expressed in regions of active neurogenesis. We addressed this question by double-labeling 24 hpf embryos for *sfpq* RNA by in situ hybridization followed by antibody labeling for HuC/D, an early marker for postmitotic neurons (Marusich et al., 1994). This confirmed that multiple regions in the brain with the strongest *sfpq* expression overlap with regions labeled with HuC/D (Fig. 4). This overlap is particularly apparent in the telencephalon (Fig. 4A,C bracket) and in the hindbrain (Fig. 4B,D bracket). A higher magnification view of the hindbrain shows two darker stripes along its anteroposterior extent, with less expression medially (Fig. 4B, dark stripe in brackets). HuC/D labeling in the hindbrain occurs only within the region of stronger *sfpq* expression (Fig. 4D).

These data show that differentiating neurons express high levels of *sfpq* in the zebrafish, and together with a report of high PSF levels in differentiating mouse brain neurons (Chanas-Sacre et al., 1999), suggest that PSF may have brain-specific activity, functioning during neuronal differentiation. However, *sfpq* is also expressed broadly during zebrafish embryonic development and in the adult, consistent with PSF expression in non-neural human and rat tissues (Shav-Tal et al., 2000; Dong et al., 2005). Reminiscent of the case for *sfpq*, the RNA binding proteins, Nova1 and Nova2, have been proposed to be brain-specific splicing factors in mammals, and aberrant splicing of neural genes is seen in Nova knockout mutants (Yang et al., 1998; Jensen et al., 2000; Ule et al., 2005). However, both Nova1 and Nova2 are also expressed in one or more non-neural tissues, including liver and lung (Buckanovich et al., 1993; Yang et al., 1998). Thus, splicing factors with tissue-specific activity may also have more general activity. This is the case for the essential splicing factor ASF/SF2, which has been implicated in cardiac-specific splicing (Xu et al., 2005b), while the ubiquitously expressed PTB, the polypyrimidine-tract–binding protein, specifically represses neuron-specific splicing of the γ-aminobutyric acid (A) receptor in non-neuronal cells (Ashiya and Grabowski, 1997).

Loss of *sfpq* Function Does Not Affect Cell Proliferation but Leads to Widespread Cell Death

While extensive in vitro analysis has shown that PSF protein can participate in a variety of functions (Shav-Tal and Zipori, 2002), loss of PSF function has not been examined in any whole animal. To characterize the PSF loss of function phenotype, we analyzed levels of cell proliferation in *wis* embryos at 24 hpf, by labeling mitotic cells with an antibody to phosphorylated histone H3 (PH3; Hendzel et al., 1997; Saka and Smith, 2001). There are no obvious differences in cell proliferation levels between *wis* mutants and their wild-type siblings (Fig. 5A,B), and quantitation of PH3-positive cells in the hindbrain and trunk region show no statistical difference between mutant and wild-type embryos ($n = 8$; $P = 0.8046$; Fig. 5C, and data not shown).

In contrast, analysis of cell death at 24 hpf by terminal deoxynucleotidyl transferase–mediated deoxyuridinetriphosphate nick end-labeling (TUNEL) labeling shows that *wis* mutants display twice the normal amount of cell death throughout the embryo (Fig. 5D–F; $n = 14$; $P < 0.0001$, and data not shown). Increased cell death continues through 2 dpf (data not shown), occurring in many tissues, even those that express *sfpq* at low levels. This finding could be due to loss of low level *sfpq* expression, or it could be a result of loss of *sfpq* at earlier time points. Regardless, these results suggest that *sfpq* is not required for regulation of cell proliferation, but is involved in regulating cell death. Several lines of evidence suggest that PSF responds to and/or can modulate apoptosis. In apoptotic cells, PSF dissociates from a partner, PTB, and binds new partners, including the splicing factors U1-70K and SR proteins (Shav-Tal et

Fig. 3. *sfpq* expression patterns. **A:** Reverse transcriptase-polymerase chain reaction (RT-PCR) for *sfpq* in embryonic tissue shows that *sfpq* is expressed beginning at 1 hpf (lane 1) and peaks at 18 hours postfertilization (hpf, lane 5). Adult tissue also has *sfpq* expression, with the brain showing the highest level (lane 11) and heart and body muscle showing lower levels (lanes 14, 15). Actin RT-PCR was used as control for RNA levels. B–Q: *sfpq* in situ hybridization time course shows that *sfpq* is expressed throughout embryogenesis. **B:** At 1 hpf (four-cell stage), side view. **C:** At 4 hpf (blastula stage), side view. **D:** At 8 hpf (75% epiboly stage), side view, dorsal right. **E:** At 12 hpf (six-somite stage), side view, dorsal right, anterior top. **F–H:** At 18 hpf, strongest expression in the forebrain (H, bracket) and in presumptive rhombomere 4 (H, arrow). **I–K:** At 24 hpf. **L–N:** At 2 dpf, expression appears restricted to strong longitudinal strips in the ventral brain (M, arrow) and in weaker transverse stripes in the hindbrain. **O–Q:** At 3 dpf, expression ventral to brain (P, arrow) and along axon tracts. F–G,I–J,L–M,O–P: Side views, anterior left. H,K,N,Q: Dorsal views, anterior left. Note: in I–Q, regions without staining may not be in focus, as to allow high magnification imaging of the stained regions. In areas of staining, the fuzziness sometimes observed is due to low levels of diffuse staining, not poor imaging. Scale bar = 100 μm.

Fig. 4. *sfpq* is strongly expressed in regions of neurogenic activity. **A–D:** At 24 hours postfertilization (hpf) wild-type embryos labeled for *sfpq* expression by in situ hybridization only (A,B) and wild-type sibling embryos double labeled for *sfpq* mRNA expression and HuC protein by immunohistochemistry (C,D) show that regions of strongest *sfpq* expression in the brain (brackets) overlap with HuC, a marker for postmitotic neuronal precursors. B,D: Higher magnification of hindbrain; brackets mark strong *sfpq* expression overlapping with HuC labeling. Midline staining is an artifact of the staining process, because it is not observed in embryos cut open before staining. A–D: Dorsal views. Anterior left. Scale bar = 100 μm.

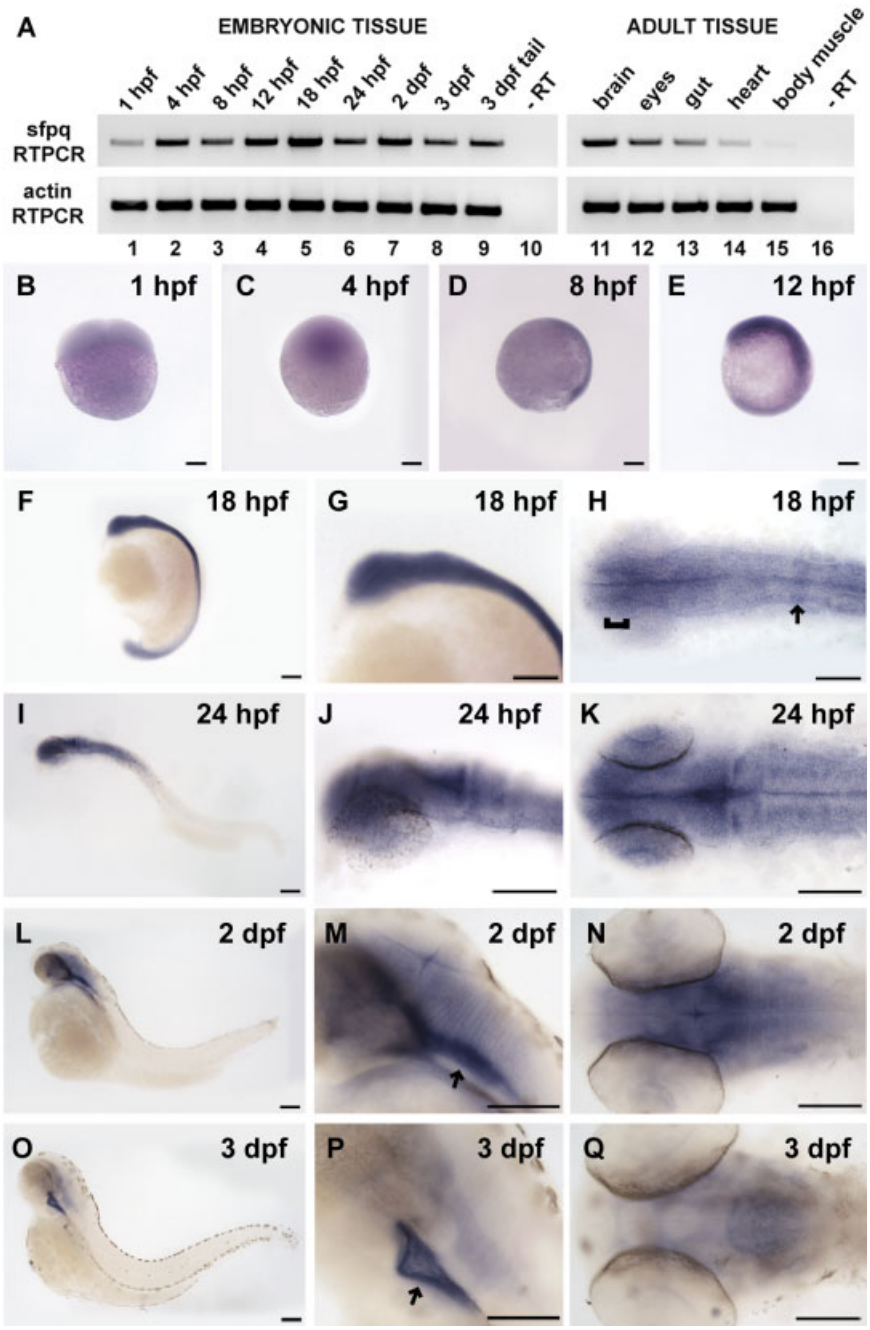

Fig. 3.

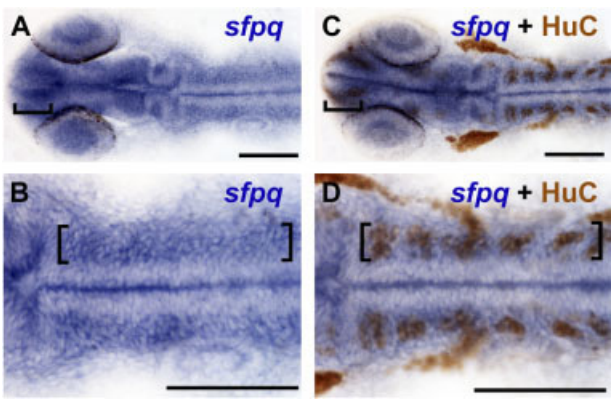

Fig. 4.

al., 2001). Additionally, during apoptosis, PSF relocalizes into globular nuclear structures, rather than in the nuclear "speckles" (interchromatin granules) normally observed (Shav-Tal et al., 2001). Of interest, PSF induces apoptosis when overexpressed in mammalian cell culture (Xu et al., 2005a), and it is not clear how this observation relates to the increase in apoptosis we observe in *wis/sfpq* mutants.

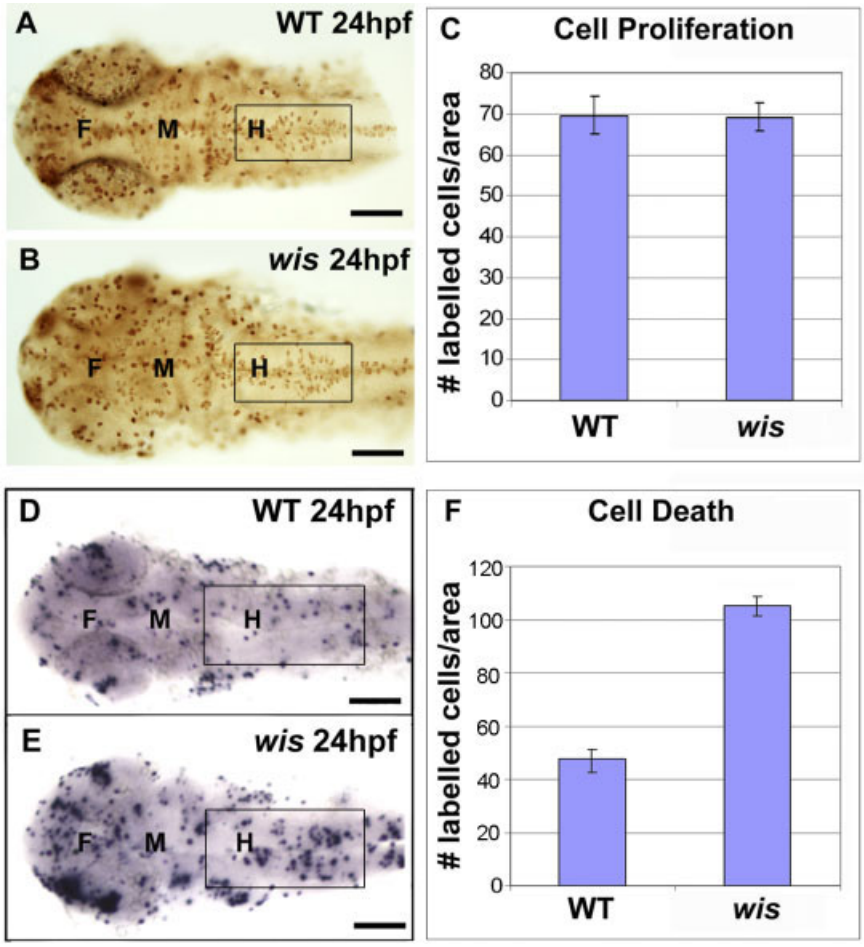

Fig. 5.

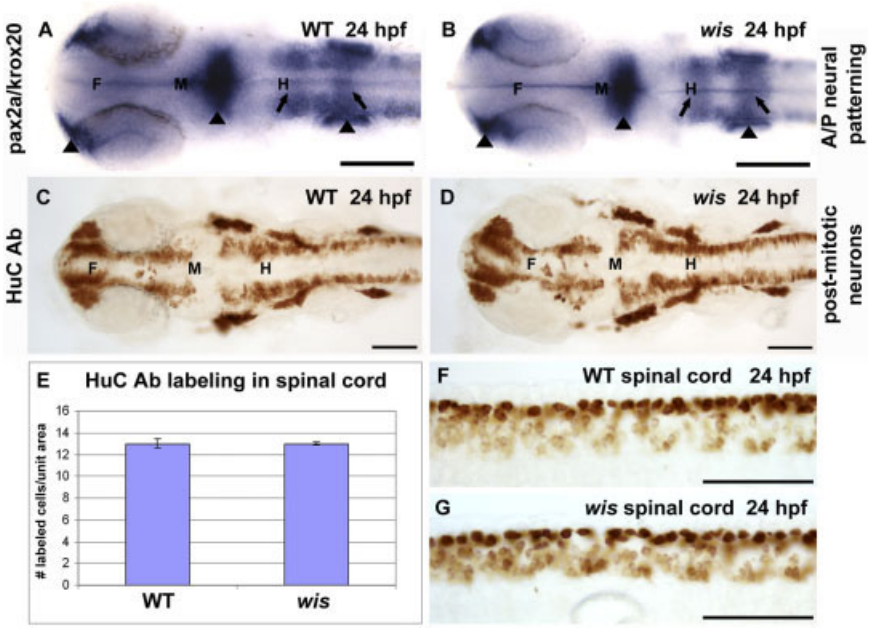

Fig. 6.

sfpq Is Required for the Differentiation, but Not Determination, of Certain Neuronal Cell Types

Because *sfpq* is strongly expressed in the brain, and particularly in determined, postmitotic neuronal precursors, we asked whether and when *sfpq* alters neuronal development. We first analyzed neural patterning in *wis* mutants at 24 hpf. Expression of the anteroposterior neural markers *krox20*, *pax2.1*, and the dorsoventral markers *opl*, and *shh* (Krauss et al., 1991, 1993; Oxtoby and Jowett, 1993; Grinblat et al., 1998) is identical in *wis* mutants and wild-type siblings (Fig. 6A,B, and data not shown), suggesting that *sfpq* is not required for early neural patterning. Second, we analyzed early neurogenesis in *wis* mutants. Expression of *zash1B*, a proneural gene expressed exclusively in cycling neural progenitors (Allende and Weinberg, 1994; Mueller and Wullimann, 2003), is similar between *wis* mutants and wild-type siblings (data not shown). Similarly, expression of

Fig. 5. Cell proliferation and cell death analysis in *whitesnake* mutants. A–C: Cell proliferation analysis, using PH3 antibody labeling. **A,B:** Fixed and labeled wild-type and *wis* brain at 24 hours postfertilization (hpf). **C:** Quantification comparing labeling in hindbrain shows no difference between wild-type and mutant, n = 8; $P = 0.8046$. D–F: Cell death analysis, using terminal deoxynucleotidyl transferase–mediated deoxyuridinetriphosphate nick end-labeling (TUNEL) staining. **D,E:** Fixed and labeled wild-type and *wis* brain at 24 hpf. **F:** Quantification comparing labeling in hindbrain shows approximately twice the amount of cell death in the mutant than in wild-type, n = 14; $P < 0.0001$. Error bars denote standard error. A–B,D–E: Dorsal views. Boxes mark regions used for quantitation. F, forebrain; M, midbrain; H, hindbrain. Scale bar = 100 μm.

Fig. 6. Neuronal determination is normal in *whitesnake* mutants. **A,B:** In situ hybridization for *pax2a* (labeling nasal placodes, midbrain–hindbrain boundary, and otic vesicles, arrowheads) and *krox20* (labeling rhombomeres 3 and 5, arrows) show similar staining patterns in wild-type and mutant. **C,D:** Immunohistochemistry for HuC, a marker for postmitotic neurons, shows identical patterns between wild-type and mutant. **E–G:** This finding has been quantified in graph E, which depicts the number of HuC-labeled cells per unit area in the spinal cords of wild-type and *wis* (F,G). F, forebrain; M, midbrain; H, hindbrain. Scale bar = 100 μm.

HuC/D, one of the earliest markers for postmitotic neuronal precursors (Marusich et al., 1994), shows no difference between *wis* and wild-type siblings (Fig. 6C–G). Quantitation of HuC/D cell labeling in the spinal cord confirms that the number of Hu-positive cells is the same between *wis* and wild-type embryos (Fig. 6E–G; n = 5; $P = 0.2672$). These results indicate that *sfpq* is not required for early neural patterning and neuronal determination and show that the number of postmitotic neuronal precursors is normal in the *wis* mutant.

In contrast, markers for later neuronal differentiation show obvious expression defects in *wis* mutants. Labeling the 24 hpf embryonic axon scaffolds with anti-acetylated tubulin or anti–HNK-1 (Metcalfe et al., 1990) demonstrates a large reduction in the number of axon tracts throughout the brain (Fig. 7A–J). Immunostaining with a monoclonal antibody directed against Neurofilament M, which labels both cell bodies and axons of hindbrain reticulospinal neuronal (Pleasure et al., 1989), shows a complete absence of all reticulospinal neurons in the hindbrain except the Mauthner neurons (Fig. 7K,L). By 2 dpf, Mauthner neurons appear somewhat abnormal, with a rounded cell body and occasional axonal pathfinding abnormalities (Fig. 7M,N, and not shown). No other hindbrain reticulospinal neurons are present. Importantly, not all neuronal cell types are affected in *wis*, as labeling with an anti-islet antibody, which marks differentiated motoneuron cell bodies (Ericson et al., 1992) shows no differences between *wis* and wild-type siblings in the brain (Fig. 7O,P) or in the spinal cord (Fig. 7Q,R). Quantitation in the brain demonstrates identical numbers of labeled cells are present in this region (n = 5; $P = 0.7517$; Supplementary Figure S2). One caveat to these conclusions is that we have analyzed survival of motoneuron cell bodies but not axons, raising the interesting possibility that cell bodies survive while axons degenerate. However, this possibility is clearly not generally true, as both cell bodies and axons were absent from *wis* reticulospinal neurons.

These data suggest that a second phase of *sfpq* function is neural-specific. In particular, only specific classes of differentiated neurons are absent in the *sfpq/wis* mutants, while other classes are present in normal numbers. Furthermore, the number of postmitotic neuronal precursors identified by HuC/D labeling is indistinguishable between wild-type and mutant at 24 hpf. Thus, even with increased cell death throughout the embryo, normal numbers of determined and postmitotic neurons are recruited. Together, the data indicate that neuronal differentiation, but not neuronal determination, requires *sfpq* function.

CONCLUSION: SEPARABLE FUNCTIONS FOR *SFPQ*?

Is the increase in cell death we observe in *sfpq/wis* mutants simply the result of removing a housekeeping function from the embryo? The notion of housekeeping functions has become complex, where some genes have both ubiquitously required functions and cell type-specific functions, such as the essential splicing factor ASF/SF2, implicated in cardiac-specific splicing (Xu et al., 2005b), and the ubiquitously expressed PTB, the polypyrimidine-tract–binding protein, which represses neuron-specific splicing in non-neuronal cells (Ashiya and Grabowski, 1997). PSF may also have both general and tissue-specific functions.

Clearly, there is an embryo-wide requirement for PSF protein. Our data suggest that PSF normally suppresses apoptosis, although the mechanisms by which it interfaces with the apoptotic machinery are not clear. A report that overexpressed PSF promotes apoptosis in mammalian tissue culture contradicts our finding in whole animals (Xu et al., 2005a) and suggests either that cells respond to either too much or too little PSF, or indicates a species-specific difference in PSF function.

Later in development, a second effect of loss of PSF function is apparent, as specific neuronal classes fail to differentiate. This finding is not a general phenotype, as formation of some neuronal classes is unaffected, while numbers of neurons in other classes are profoundly decreased or are absent. Consistent with two phases of *sfpq* function is the replacement of low level, ubiquitous early expression of *sfpq* with later and very strong expression that is enriched in developing brain relative to the rest of the embryo. This finding suggests separable early and late functions for *sfpq*. Our data are consistent with other reports that demonstrate PSF has numerous cellular functions (Shav-Tal and Zipori, 2002).

Is specific neuronal loss linked to the effects of PSF on apoptosis? We cannot yet distinguish whether particular neuronal classes are absent because they do not survive or because they cannot differentiate. This question will be best answered by defining whether neuronal progenitors die in *spfq/wis* mutants. Definition of PSF target genes will also help answer this question. An alternate explanation is that another function of PSF is necessary for differentiation of specific neuronal classes. In particular, PSF could play a role in brain-specific splicing or transcriptional regulation. *whitesnake/sfpq* mutants will be indispensable tools to investigate whether PSF function depends on its splicing activity or on another function of this protein, and to characterize potential targets of PSF.

EXPERIMENTAL PROCEDURES

Fish Lines and Maintenance

Danio rerio were raised and bred according to standard methods (Westerfield, 1995). Embryos were kept at 28.5°C and staged according to Kimmel et al. (1995). Times of development are expressed as hours postfertilization (hpf) or days postfertilization (dpf).

Lines used were AB, Tübingen Long Fin, $sfpq^{hi1779}$ (Amsterdam et al., 2004), wis^{tr241} (Jiang et al., 1996), and wis^{m427} (Schier et al., 1996). For PCR genotyping, tails or embryos were digested with proteinase K (1 mg/ml) in lysis buffer (10 mmol/L Tris pH 8, 1 mmol/L ethylenediaminetetraacetic acid, 0.3% Tween-20, 0.3% NP40). Because $sfpq^{hi1779}$ has a retroviral insertion in the *sfpq* gene, mutant individuals could be identified by PCR. Primers used are as follows: 1779c, 5′-cagcagactcccaccgtcg-3′; MSL4, 5′-gctagcttgccaaacctacaggt-3′ (MWG Biotech).

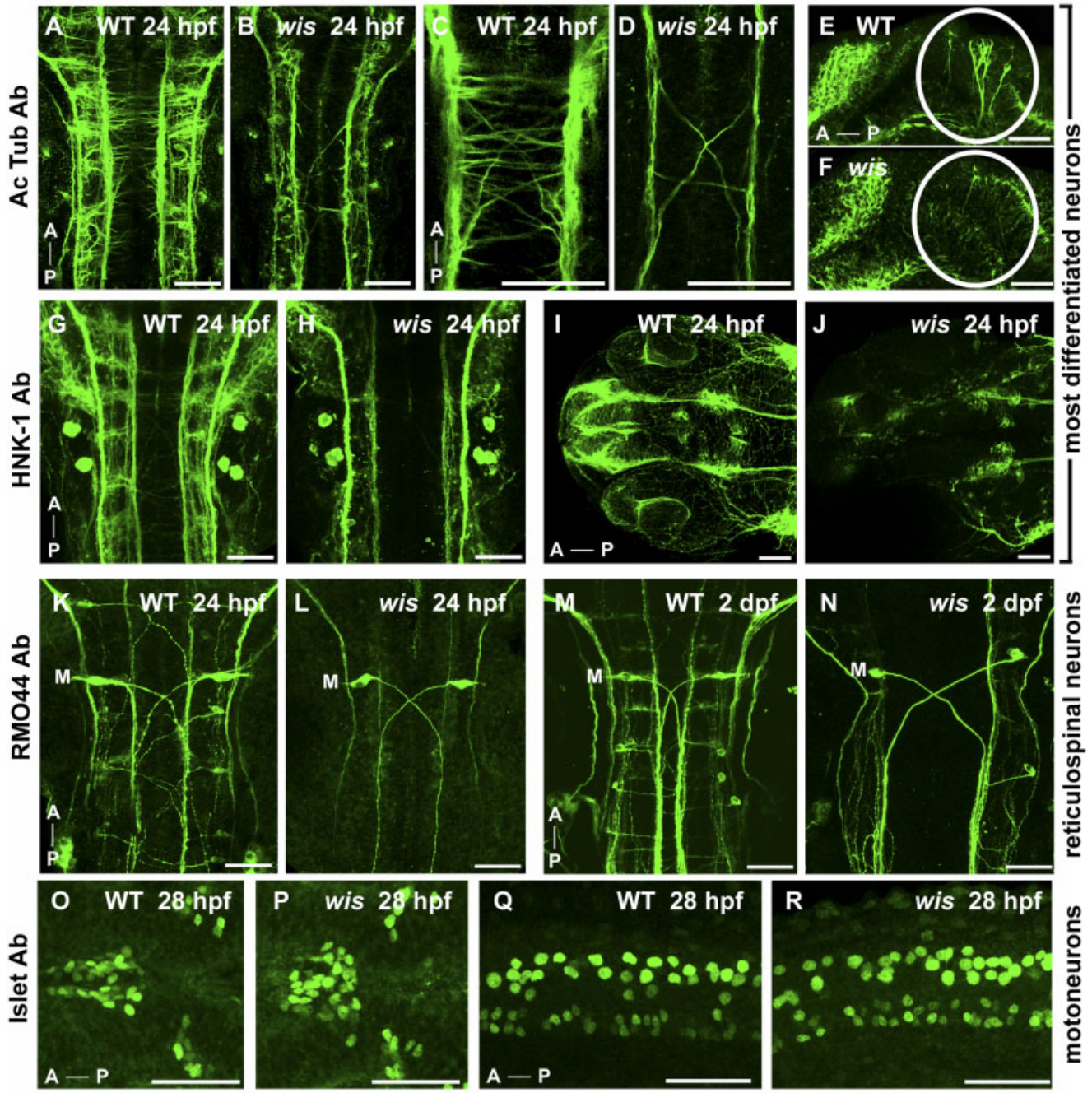

Fig. 7. Specific neurons are absent in *whitesnake* mutants. **A–J:** Acetylated tubulin antibody labeling (A–F) and HNK-1 antibody labeling (G–J), both of which mark most differentiated neurons and their axons, show reduced number of axons in *wis* mutant in the hindbrain (B,D,H), midbrain (F), and eyes/forebrain (J) compared with wild-type (A,C,E,G,I). **K–N:** The RM044 Ab, which labels reticulospinal neurons, shows an absence of all reticulospinal neurons in the *wis* hindbrain except Mauthner neurons (labeled with M) at both 24 hours postfertilization (hpf, L) and 2 days postfertilization (dpf, N), compared with wild-type (K,M). **O–R:** The 4D5 Islet antibody, labeling motoneurons, shows no loss of motoneurons in *whitesnake* in the dorsal diencephalon (P) or spinal cord (R) compared with wild-type (O,Q). A, anterior; P, posterior. A–D,G–P: Dorsal views. E–F,Q–R: Side views. Scale bar = 50 μm.

MSL4 detects the retroviral insertion, which is located 553 base pairs downstream from the *sfpq* start site in the *hi1779* mutant. The C to T mutation present in wis^{tr241} introduces an *Acc*I restriction site and, thus, can be detected by PCR followed by digestion. All procedures on live animals and embryos were approved by the Massachusetts Institute of Technology Committee on Animal Care.

Brain Ventricle Imaging

Methods for brain ventricle imaging have been described previously (Lowery and Sive, 2005). Briefly, embryos were anesthetized in 0.1 mg/ml Tricaine (Sigma) dissolved in embryo medium before hindbrain ventricle microinjection with 2–10 nl of dextran conjugated to Rhodamine (5% in 0.2 mol/L KCl, Sigma), and then embryos were imaged by light and fluorescence

microscopy with a Leica dissecting microscope, using a KT Spot Digital Camera (RT KE Diagnostic Instruments). Images were superimposed in Photoshop 6 (Adobe).

Detection of *whitesnake* Mutation

Total RNA was extracted from mutant embryos and wild-type siblings using Trizol reagent (Invitrogen), followed by chloroform extraction and isopropanol precipitation. cDNA synthesis was performed with Super Script II Reverse Transcriptase (Invitrogen) and random hexamers. PCR was then performed using five sets of primers, which amplify the coding region of *sfpq*. Primers used are as follows: sfpq1F, 5′-tgagggtgctcctctctttg -3′; sfpq1R, 5′- gagagcgttgccttcaattc-3′; sfpq2F, 5′-tccaccgaagatccagtctc-3′; sfpq2R, 5′-ggcagctggcttagaagaaa-3′; sfpq3F, 5′-gaggttgcgaaagcagagtt-3′; sfpq3R, 5′-tcatctcctcctctctcctacg-3′; sfpq4F, 5′-aggcagcaagtggagaaaaa-3′; sfpq4R, 5′-gccacaaatgggatgagttt-3′; sfpq5F, 5′-gcaaacgcgaggaatcttac-3′; sfpq5R, 5′-tttttgggagaaccaactgc-3′. RT-PCR products were used for sequencing analysis, performed by Northwoods DNA, Inc. (Solway MN). Sequencing data was analyzed using the BLAST program (http://www.ncbi.nlm.nih.gov/BLAST/), and the cDNA sequence of *sfpq* was obtained from the GenBank database (NM_213278).

RNA Injections

Full-length *sfpq* cDNAs were generated by RT-PCR with primers, including *Cla*I/*Xba*1 sites, *Cla*I-sfpq1F 5′-cc**at/cgat**tgagggtgctcctctctttg-3′; *Xba*I-sfpq5R 5′-gc**t/ctaga**tttttgggagaaccaactgc-3′. The PCR fragments were subcloned into pCS2+, and the pCS2+ constructs were linearized by *Not*I. Capped mRNA was transcribed in vitro using the SP6 mMessage mMachine kit (Ambion). Embryos were injected at the one-cell stage with 100–300 pg of mRNA. The embryos phenotypically rescued by mRNA injection were identified as mutants by genotyping.

Morpholino Oligo Injections

A morpholino antisense oligonucleotide (MO) targeted to the translation start site of zebrafish *sfpq* (5′-ccatgccaccgcgcatccccattcc-3′) was injected into one- to two-cell embryos. The final amounts used were 8 ng of *sfpq* or control MO (provided by Gene Tools, Inc.).

RT-PCR Time Course

Total RNA was extracted from staged wild-type embryos or adult dissected tissue using Trizol reagent (Invitrogen), followed by chloroform extraction and isopropanol precipitation. cDNA synthesis was performed with Super Script II Reverse Transcriptase (Invitrogen) and random hexamers. PCR was then performed using sfpq4F and sfpq4R (listed above), and actinF 5′-tatccacgagaccaccttcaactcc-3′, actinR 5′-ctgcttgctgatccacatctgctgg-3′.

In Situ Hybridization

RNA probes containing digoxigenin (DIG) -11-UTP were synthesized from linearized plasmid DNA for *sfpq*, *pax2.1* (Krauss et al., 1991), *krox20* (Oxtoby and Jowett, 1993), *opl* (Grinblat et al., 1998), *shh* (Krauss et al., 1993), and *zash1B* (Allende and Weinberg, 1994) as described (Harland, 1991). Standard methods for hybridization and for single color labeling were used as described elsewhere (Sagerstrom et al., 1996). After staining, embryos were fixed in 4% paraformaldehyde overnight at 4°C, washed in phosphate buffered saline (PBS), dehydrated in methanol, and then cleared in a 3:1 benzyl benzoate/benzyl alcohol (BB/BA) solution before mounting and imaging with a Nikon compound microscope.

Immunohistochemistry

Whole-mount immunostaining was carried out using rabbit anti-phosphohistone H3 (Upstate Biotechnology, 1:800), mouse anti-acetylated tubulin (Sigma, 1:1,000), mouse anti-neurofilament RM044 (Zymed #13-0500, 1:50), mouse HNK-1/zn-12 (Zebrafish International Resource Center, 1:500), mouse 39.4D5 anti-islet (Developmental Studies Hybridoma Bank, 1:100), mouse anti-HuC (Molecular Probes, 1:500), and mouse MF20 IgG2b (Developmental Studies Hybridoma Bank, 1:10). Goat anti-rabbit IgG Alexa Fluor 488 (Molecular Probes, 1:500), goat anti-mouse Alexa Fluor 488 (Molecular Probes, 1:500), goat anti-mouse IgG horseradish peroxidase (HRP; Sigma, 1:500), goat anti-rabbit IgG HRP (Sigma, 1:500), and goat anti-mouse IgG2b Alexa Fluor 568 (Molecular Probes, 1:500) were used as secondary antibodies.

For labeling with anti-phosphohistone H3, anti-acetylated tubulin, HNK-1 antibody, 39.4D5 antibody, anti-HuC, and MF20 antibody, dechorionated embryos were fixed in 4% paraformaldehyde for 2 hr at room temperature, then rinsed in PBS. For anti-phosphohistone H3 and anti-HuC, endogenous peroxidase activity was quenched in 10% hydrogen peroxide in PBT for 1 hr. For all antibodies, blocking was done for 4 hr at room temperature in 0.5% Triton X, 4% normal goat serum, in phosphate buffer. Detection of HRP was performed with the diaminobenzidine substrate peroxidase kit (Vector Laboratories). Fluorescent secondary antibodies were visualized by confocal microscopy (LSM510). Brains were flat-mounted in glycerol and imaged. Images are composites of several scans.

For labeling with RM044 antibody, dechorionated embryos were fixed in 2% tricloroacetic acid 3 hr at room temperature, washed in PBS, blocked in 10% normal goat serum in PBT for 3 hr before incubation in antibody. The brains were partially dissected and mounted for visualization by confocal microscopy. To block pigmentation, embryos were incubated in 0.2 mM 1-phenyl-2-thiorurea in embryo medium beginning at 22 hpf.

Cell Death Labeling

DNA fragmentation during apoptosis was detected by the TUNEL method, using 'ApopTag' kit (Chemicon). Embryos were fixed in 4% paraformaldehyde in PBS for 2 hr, then rinsed in PBS and dechorionated. Embryos were dehydrated to 100% ethanol, stored at −20°C overnight, then rehydrated in PBS. Embryos were further permeabilized by incubation in proteinase K (5 μg/ml) for 5 min, then rinsed in PBS. TdT labeling was followed per manufacturer's instructions. Anti–DIG-AP (Gibco, 1:100) was used to detect the DIG-labeled ends.

Brains were flat-mounted in glycerol and imaged.

Statistical Analysis

To quantify amount of cell proliferation, cell death, or antibody staining, labeled cells in a defined area of the brain and/or tail were counted and then compared statistically using an unpaired *t*-test (InStat v.3, GraphPad software).

ACKNOWLEDGMENTS

We thank members of the Sive Lab for helpful comments and Olivier Paugois for fish husbandry. Many thanks to the Nusslein-Volhard lab for providing us with the *wis tr241* mutant, the Zebrafish International Resource Center for the *wis m427* mutant and zn-12 antibody, Adam Amsterdam and Nancy Hopkins for *sfpq hi1779* mutant. The 39.4D5 antibody developed by Thomas Jessell, and the MF20 antibody developed by Donald Fischman, were obtained from the Developmental Studies Hybridoma Bank developed under the auspices of the NICHD and maintained by the University of Iowa, Department of Biological Sciences (Iowa City, IA). This work was conducted using the W.M. Keck Foundation Biological Imaging Facility at the Whitehead Institute. The Zebrafish International Resource Center is supported by the NIH-NCRR. H.S. is supported by NIH. L.A.L. is supported by NIH NRSA predoctoral fellowship and an Abraham J. Siegel Fellowship at the Whitehead Institute.

REFERENCES

Allende ML, Weinberg ES. 1994. The expression pattern of two zebrafish achaete-scute homolog (ash) genes is altered in the embryonic brain of the cyclops mutant. Dev Biol 166:509–530.

Amsterdam A, Nissen RM, Sun Z, Swindell EC, Farrington S, Hopkins N. 2004. Identification of 315 genes essential for early zebrafish development. Proc Natl Acad Sci U S A 101:12792–12797.

Ashiya M, Grabowski PJ. 1997. A neuron-specific splicing switch mediated by an array of pre-mRNA repressor sites: evidence of a regulatory role for the polypyrimidine tract binding protein and a brain-specific PTB counterpart. RNA 3: 996–1015.

Buckanovich RJ, Posner JB, Darnell RB. 1993. Nova, the paraneoplastic Ri antigen, is homologous to an RNA-binding protein and is specifically expressed in the developing motor system. Neuron 11: 657–672.

Chanas-Sacre G, Mazy-Servais C, Wattiez R, Pirard S, Rogister B, Patton JG, Belachew S, Malgrange B, Moonen G, Leprince P. 1999. Identification of PSF, the polypyrimidine tract-binding protein-associated splicing factor, as a developmentally regulated neuronal protein. J Neurosci Res 57:62–73.

Clark J, Lu YJ, Sidhar SK, Parker C, Gill S, Smedley D, Hamoudi R, Linehan WM, Shipley J, Cooper CS. 1997. Fusion of splicing factor genes PSF and NonO (p54nrb) to the TFE3 gene in papillary renal cell carcinoma. Oncogene 15:2233–2239.

Dong X, Shylnova O, Challis JR, Lye SJ. 2005. Identification and characterization of the protein-associated splicing factor as a negative co-regulator of the progesterone receptor. J Biol Chem 280:13329–13340.

Dye BT, Patton JG. 2001. An RNA recognition motif (RRM) is required for the localization of PTB-associated splicing factor (PSF) to subnuclear speckles. Exp Cell Res 263:131–144.

Emili A, Shales M, McCracken S, Xie W, Tucker PW, Kobayashi R, Blencowe BJ, Ingles CJ. 2002. Splicing and transcription-associated proteins PSF and p54nrb/nonO bind to the RNA polymerase II CTD. RNA 8:1102–1111.

Ericson J, Thor S, Edlund T, Jessell TM, Yamada T. 1992. Early stages of motor neuron differentiation revealed by expression of homeobox gene Islet-1. Science 256:1555–1560.

Grinblat Y, Gamse J, Patel M, Sive H. 1998. Determination of the zebrafish forebrain: induction and patterning. Development 125:4403–4416.

Harland RM. 1991. In situ hybridization: an improved whole-mount method for Xenopus embryos. Methods Cell Biol 36: 685–695.

Hendzel MJ, Wei Y, Mancini MA, Van Hooser A, Ranalli T, Brinkley BR, Bazett-Jones DP, Allis CD. 1997. Mitosis-specific phosphorylation of histone H3 initiates primarily within pericentromeric heterochromatin during G2 and spreads in an ordered fashion coincident with mitotic chromosome condensation. Chromosoma 106:348–360.

Jensen KB, Dredge BK, Stefani G, Zhong R, Buckanovich RJ, Okano HJ, Yang YY, Darnell RB. 2000. Nova-1 regulates neuron-specific alternative splicing and is essential for neuronal viability. Neuron 25:359–371.

Jiang YJ, Brand M, Heisenberg CP, Beuchle D, Furutani-Seiki M, Kelsh RN, Warga RM, Granato M, Haffter P, Hammerschmidt M, Kane DA, Mullins MC, Odenthal J, van Eeden FJ, Nusslein-Volhard C. 1996. Mutations affecting neurogenesis and brain morphology in the zebrafish, Danio rerio. Development 123: 205–216.

Kimmel CB, Ballard WW, Kimmel SR, Ullmann B, Schilling TF. 1995. Stages of embryonic development of the zebrafish. Dev Dyn 203:253–310.

Krauss S, Johansen T, Korzh V, Fjose A. 1991. Expression of the zebrafish paired box gene pax[zf-b] during early neurogenesis. Development 113:1193–1206.

Krauss S, Concordet JP, Ingham PW. 1993. A functionally conserved homolog of the Drosophila segment polarity gene hh is expressed in tissues with polarizing activity in zebrafish embryos. Cell 75: 1431–1444.

Lowery LA, Sive H. 2005. Initial formation of zebrafish brain ventricles occurs independently of circulation and requires the nagie oko and snakehead/atp1a1a.1 gene products. Development 132:2057–2067.

Marusich MF, Furneaux HM, Henion PD, Weston JA. 1994. Hu neuronal proteins are expressed in proliferating neurogenic cells. J Neurobiol 25:143–155.

Metcalfe WK, Myers PZ, Trevarrow B, Bass MB, Kimmel CB. 1990. Primary neurons that express the L2/HNK-1 carbohydrate during early development in the zebrafish. Development 110:491–504.

Mueller T, Wullimann MF. 2003. Anatomy of neurogenesis in the early zebrafish brain. Brain Res Dev Brain Res 140:137–155.

Oxtoby E, Jowett T. 1993. Cloning of the zebrafish krox-20 gene (krx-20) and its expression during hindbrain development. Nucleic Acids Res 21:1087–1095.

Patton JG, Porro EB, Galceran J, Tempst P, Nadal-Ginard B. 1993. Cloning and characterization of PSF, a novel pre-mRNA splicing factor. Genes Dev 7:393–406.

Pleasure SJ, Selzer ME, Lee VM. 1989. Lamprey neurofilaments combine in one subunit the features of each mammalian NF triplet protein but are highly phosphorylated only in large axons. J Neurosci 9:698–709.

Sagerstrom CG, Grinbalt Y, Sive H. 1996. Anteroposterior patterning in the zebrafish, Danio rerio: an explant assay reveals inductive and suppressive cell interactions. Development 122:1873–1883.

Saka Y, Smith JC. 2001. Spatial and temporal patterns of cell division during early Xenopus embryogenesis. Dev Biol 229:307–318.

Schier AF, Neuhauss SC, Harvey M, Malicki J, Solnica-Krezel L, Stainier DY, Zwartkruis F, Abdelilah S, Stemple DL, Rangini Z, Yang H, Driever W. 1996. Mutations affecting the development of the embryonic zebrafish brain. Development 123:165–178.

Shav-Tal Y, Zipori D. 2002. PSF and p54(nrb)/NonO—multi-functional nuclear proteins. FEBS Lett 531:109–114.

Shav-Tal Y, Lee B, Bar-Haim S, Vandekerckhove J, Zipori D. 2000. Enhanced proteolysis of pre-mRNA splicing factors in

myeloid cells. Exp Hematol 28:1029–1038.

Shav-Tal Y, Cohen M, Lapter S, Dye B, Patton JG, Vandekerckhove J, Zipori D. 2001. Nuclear relocalization of the pre-mRNA splicing factor PSF during apoptosis involves hyperphosphorylation, masking of antigenic epitopes, and changes in protein interactions. Mol Biol Cell 12:2328–2340.

Ule J, Ule A, Spencer J, Williams A, Hu JS, Cline M, Wang H, Clark T, Fraser C, Ruggiu M, Zeeberg BR, Kane D, Weinstein JN, Blume J, Darnell RB. 2005. Nova regulates brain-specific splicing to shape the synapse. Nat Genet 37:844–852.

Westerfield M. 1995. The Zebrafish book: a guide for the laboratory use of zebrafish. Eugene: University of Oregon Press.

Xu J, Zhong N, Wang H, Elias JE, Kim CY, Woldman I, Pifl C, Gygi SP, Geula C, Yankner BA. 2005a. The Parkinson's disease-associated DJ-1 protein is a transcriptional co-activator that protects against neuronal apoptosis. Hum Mol Genet 14:1231–1241.

Xu X, Yang D, Ding JH, Wang W, Chu PH, Dalton ND, Wang HY, Bermingham JR Jr, Ye Z, Liu F, Rosenfeld MG, Manley JL, Ross J, Jr., Chen J, Xiao RP, Cheng H, Fu XD. 2005b. ASF/SF2-regulated CaMKIIdelta alternative splicing temporally reprograms excitation-contraction coupling in cardiac muscle. Cell 120:59–72.

Yang YY, Yin GL, Darnell RB. 1998. The neuronal RNA-binding protein Nova-2 is implicated as the autoantigen targeted in POMA patients with dementia. Proc Natl Acad Sci U S A 95:13254–13259.